

# Deformation-Induced Color Changes in Mechanochromic Polyethylene Blends

Brent R. Crenshaw, Mark Burnworth, Devang Khariwala, Anne Hiltner,  
Patrick T. Mather, Robert Simha, and Christoph Weder\*

Department of Macromolecular Science and Engineering, Case Western Reserve University,  
2100 Adelbert Road, Cleveland, Ohio 44106-7202

Received December 21, 2006; Revised Manuscript Received January 25, 2007

**ABSTRACT:** A detailed and systematic investigation of mechanochromic, melt-processed blends between a series of polyethylenes (PE) with crystallinities ranging from 9 to 66% and two excimer-forming, photoluminescent oligo(phenylenevinylene) dyes is described. A dramatic increase in the nucleation rate of dye aggregates, and therewith a decrease in the size of the aggregates, is observed upon grafting long alkyl tails onto the chromophore. The extent of color change observed upon deformation of these materials, and thus the ability of the polymer host to break up dye aggregates upon deformation, is related to the plastic deformation process of PE crystallites—specifically those arranged in a lamellar morphology—and increases with increasing polymer crystallinity, decreasing dye aggregate size, and decreasing rates of deformation.

## Introduction

We recently reported on a new class of “self-assessing” polymers with built-in deformation sensors.<sup>1–5</sup> These materials are produced by incorporating trace amounts of excimer-forming,<sup>6,7</sup> photoluminescent (PL) chromophores into ductile host polymers via conventional melt-processing techniques. Our design relies on the initial formation of nanoscale aggregates of the sensor molecules in the polymer matrix and exploits deformation-induced transformation of the nanophase-separated systems into molecular mixtures, concomitant with a pronounced shift from excimer- to monomer-dominated emission.<sup>8</sup> The excimer-forming dyes employed in our ongoing studies are cyano-substituted oligo(*p*-phenylenevinylene) derivatives (cyano-OPVs, Figure 1).<sup>3,9</sup> These chromophores are particularly attractive for mechanochromic sensing since they often exhibit a strong tendency toward excimer formation, and the fluorescence maxima of their molecular solutions (monomer emission) and aggregates (excimer emission) display exceedingly large differences of up to 140 nm.<sup>9–18</sup> In addition, their optical characteristics and solubility in different host polymers are readily controlled by the composition and architecture of the substituents attached to the aromatic rings.<sup>3,9</sup> Our previous work in this area involved both physical mixtures of the sensor dyes with ductile semicrystalline<sup>1–3,5</sup> and glassy amorphous materials<sup>3</sup> as well as copolymers in which the dye moieties are covalently incorporated into the backbone of thermoplastic polyurethane elastomers in which the sensing effect could be exploited in the rubbery amorphous state.<sup>4</sup> Recently, we further extended the sensing concepts to include dyes that change their absorption, rather than PL emission, color.<sup>5</sup>

During our initial studies<sup>2</sup> we investigated mechanochromic blends formed by the incorporation of 1,4-bis( $\alpha$ -cyano-4-methoxystyryl)-2,5-dimethoxybenzene<sup>9</sup> (**C1-RG**, Figure 1) into a linear low-density polyethylene (LLDPE) of moderately high density ( $0.94 \text{ g cm}^{-3}$ ). In samples that were slowly cooled from the melt and which comprised the dye at a concentration that would dictate phase separation above the crystallization temperature of the LLDPE, large-scale phase separation (dye crystal size of the order of  $10 \mu\text{m}$ ) was observed during cooling, and the resulting material did not display the desired mechanochrom-

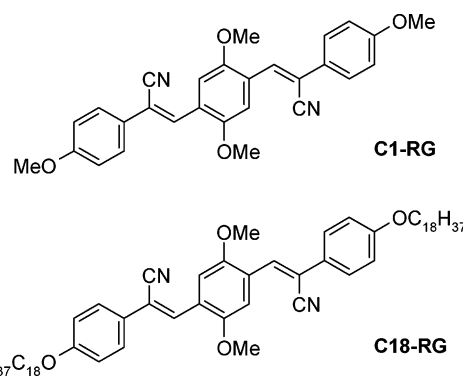


**Figure 1.** Chemical structures of 1,4-bis( $\alpha$ -cyano-4-methoxystyryl)-2,5-dimethoxybenzene (**C1-RG**) and 1,4-bis( $\alpha$ -cyano-4-octadecyloxy-styryl)-2,5-dimethoxybenzene (**C18-RG**), the cyano-OPVs employed in this study.

mic effect.<sup>2</sup> Conversely, no dye aggregates could be discerned by optical microscopy in blends that were quenched from molecularly mixed melts. These samples displayed a pronounced mechanochromic effect, which we related to the formation of nanoscale aggregates of the sensor molecules in the polymer matrix, which could be transformed into molecular mixtures upon deformation. In these blends, we observed that a significant portion of the chromophores aggregated immediately upon quenching, but the aggregation process continued over the course of a few months.<sup>2</sup> With the notion that this aging process could be driven by aggregate nucleation as well as diffusion/growth processes, we conducted a preliminary study regarding the effect of host polymer crystallinity. A similar but much faster aging process was observed for a quenched blend of **C1-RG** and a LLDPE of lower density ( $0.90 \text{ g cm}^{-3}$ ). Rather interestingly, the resulting materials displayed hardly any color change upon deformation. Motivated by the desire to develop a better understanding of the structure–property relationships in these systems, specifically with respect to aggregate size and the relation between stress, strain, and color change, and to gain further insights into the mechanism of the deformation-induced color change observed in these blends, we here report a detailed and systematic investigation

of blends between a series of PEs with different crystallinity and two cyano-OPVs.

## Experimental Section

**Materials.** 1,4-Bis( $\alpha$ -cyano-4-methoxystyryl)-2,5-dimethoxybenzene<sup>9</sup> (**C1-RG**) and 1,4-bis( $\alpha$ -cyano-4-octadecyoxystyryl)-2,5-dimethoxybenzene<sup>3</sup> (**C18-RG**) were prepared as described before. The different grades of polyethylene (PE) used in this study are referred to as **PE** $\rho$ , where  $\rho$  denotes the density of the melt-processed, quenched polymer as measured by us in an isopropanol-distilled water gradient column calibrated with glass floats. An average of at least three samples was used and we elected to employ 0.15% w/w **PE/C1-RG** blends rather than the neat PE to establish the PE densities; the measured values are in good agreement with the values reported for neat PE of similar composition.<sup>19</sup> Crystallinities were calculated from the measured densities assuming a two-phase model for PE with crystalline and amorphous densities of 1.000 and 0.855 g cm<sup>-3</sup> and omitting the contribution of the dye.<sup>20</sup> The PEs used in our study include **PE95** (Stamylan 7048, density  $\rho = 0.951$ , crystallinity  $x_c = 66\%$ ), a high-density polyethylene obtained from DSM Polymers, as well as **PE94** (Dowlex BG 2340,  $\rho = 0.939$ ,  $x_c = 58\%$ ), **PE92** (Dowlex NG 5056E,  $\rho = 0.918$ ,  $x_c = 44\%$ ), **PE90** (Attane SL 4102,  $\rho = 0.908$ ,  $x_c = 36\%$ ), and **PE87** (14.7 mol % octene,  $\rho = 0.868$ ,  $x_c = 9\%$ ). These PE samples (except for PE 95) are homogeneous LLDPEs containing different amounts of octene as a comonomer and were obtained from the Dow Chemical Co.

**Film Preparation.** Binary blends of PE and **C1-RG** or **C18-RG** containing between 0.1 and 1.0% w/w dye were prepared by feeding the appropriate amount of dye and 3.0 g of PE into a recirculating, corotating twin-screw mini-extruder (DACA Instruments, Santa Barbara, CA), mixing at ca. 100 rpm for 3 min at 180 °C, and subsequent extrusion. Films were prepared by compression-molding the blends between two aluminum foils (Kapton films were used for AFM studies) in a Carver press at 180 °C for ~3 min, using four 60  $\mu$ m spacers. After removal from the hot press the samples were immediately quenched by immersion in an ice–water bath. Blends used in tensile deformation experiments were aged at room temperature for at least 2 weeks prior to use. In comparative experiments, similar molar concentrations, specified later, of the two dyes were used to minimize potential effects that could arise from different dye concentrations.

**Optical and Optomechanical Spectroscopy.** Steady-state PL spectra were acquired on a SPEX Fluorolog FL3-12. Spectra were collected under excitation at 435 nm and were corrected for instrument throughput and detector response. In-situ optomechanical studies were carried out on an Anton-Paar rheometer (MCR-501) equipped with an Expansion Instruments SER Universal Testing Platform, which is described in detail elsewhere,<sup>21</sup> in connection with an Ocean Optics ACD1000-USB spectrometer under excitation at 480 nm. Unless otherwise noted, the emission spectra acquired by in-situ measurements were not corrected. For in-situ optomechanical experiments, film samples were cut into 4–6 mm wide strips which were notched with a 5/8 in. round stencil on both edges, leaving a 2.0 mm gap between the notches. This geometry ensured that the samples yielded in a predefined central position without causing them to fail at low strains. Unless otherwise noted, films were strained at a rate of 0.05 s<sup>-1</sup>. Strains reported in figures containing stress–strain–PL plots (and in the text when referring to these figures) are nominal values and are calculated from the angular rotation of the SER fixture’s drums.<sup>21</sup> Local strains may be different than these nominal values. Strains reported for films that were manually stretched have been measured by the displacement of ink marks on the samples.

**Atomic Force Microscopy.** Atomic force microscopy (AFM) experiments were performed on the free surfaces of as-prepared films using a Nanoscope IIIa equipped with a MultiMode head and J-scanner. All AFM measurements were conducted in tapping mode under ambient conditions. Commercial Si probes were chosen with a resonance frequency of ca. 300 kHz. Height and phase images

were recorded simultaneously. In the phase images high-modulus materials appear brighter than low-modulus materials.

## Results and Discussion

**Materials.** In order to systematically study the influence of the PE matrix on the aggregate formation of physically incorporated cyano-OPV sensor molecules and the mechanically induced dispersion of the latter, we elected to use a series of PEs spanning a large crystallinity range of between  $x_c = 66\%$  (**PE95**, a high-density PE) and 9% (**PE87**, a LLDPE with high octene comonomer content). The different grades of PE are referred to as **PE** $\rho$ , where  $\rho$  denotes the density of melt-processed, quenched samples. In addition to **PE95** and **PE87** we employed **PE94** ( $\rho = 0.939$ ,  $x_c = 58\%$ ), the LLDPE used in our previous studies,<sup>2,9</sup> as well as **PE92** ( $\rho = 0.918$ ,  $x_c = 44\%$ ) and **PE90** ( $\rho = 0.908$ ,  $x_c = 36\%$ ), which are both LLDPEs of intermediate density. The cyano-OPVs used here feature the same chromophore unit (Figure 1) and include the previously studied 1,4-bis( $\alpha$ -cyano-4-methoxystyryl)-2,5-dimethoxybenzene<sup>9</sup> (**C1-RG**) as well as 1,4-bis( $\alpha$ -cyano-4-octadecyoxystyryl)-2,5-dimethoxybenzene<sup>3</sup> (**C18-RG**). The hydrophobic octadeoxyloxy chains on **C18-RG** were originally introduced to decrease the dye’s solubility in polar host polymers such as polyesters.<sup>3</sup> On the basis of previous studies, which compared the nucleation rate of flexible molecules and their rigid counterparts,<sup>22–26</sup> and our qualitative observation of a much smaller crystal size in crystallization attempts, we surmised that the aggregation behavior of **C18-RG** in PE might be rather different from that of **C1-RG**, and we therefore included this chromophore in the present study.

Binary blend films between the PEs and these dyes were prepared by melt-mixing the components at 180 °C, compression molding at the same temperature, and quenching to 0 °C, in order to minimize the extent of large-scale phase separation between dye and polymer host (vide infra).<sup>2</sup> All blend films thus produced exhibited emission spectra comprised of both monomer emission with maxima  $\lambda_{\text{max}}$  at 495 and 537 nm and excimer emission with a  $\lambda_{\text{max}}$  at 650 nm (Figure 2a,b). Unless otherwise noted, the samples were aged at ambient conditions for at least 2 weeks prior to use. The equilibrium room temperature solubility of both **C1-RG** and **C18-RG** in **PE94** is of the order of 0.001–0.005% w/w (Supporting Information) and is expected to be similar in the other PEs. Thus, the compositions of all samples investigated in this study dictate phase separation under thermodynamic equilibrium conditions at ambient temperature.

**Aging of Melt-Processed Polyethylene/Cyano-OPV Blend Films.** In order to develop a more quantitative understanding of the aging phenomenon previously observed in quenched PE/**C1-RG** blends (vide supra) and to determine how this process is influenced by the host polymer crystallinity, we investigated the PL emission characteristics of films of a series of blends containing 0.15% w/w **C1-RG** as a function of time. For this study we selected the matrix in which the aging process was first observed (**PE94**,  $x_c = 58\%$ ),<sup>2</sup> along with **PE95** and **PE90**, which exhibit higher and lower degrees of crystallinity ( $x_c = 66\%$  and 36%, respectively). Representative PL spectra for the **PE94/C1-RG** blend are shown in Figure 2a. Following the trend observed for a similar composition before,<sup>2</sup> the ratio of monomer ( $I_M$ , 537 nm) to excimer ( $I_E$ , 650 nm) emission intensity,  $I_M/I_E$ , decreased as a function of time. As can be seen from Figure 2a, the rate of this process decreases sharply as a function of time and appears to approach zero after a time frame of a few weeks. Blends based on **PE95** and **PE90** qualitatively

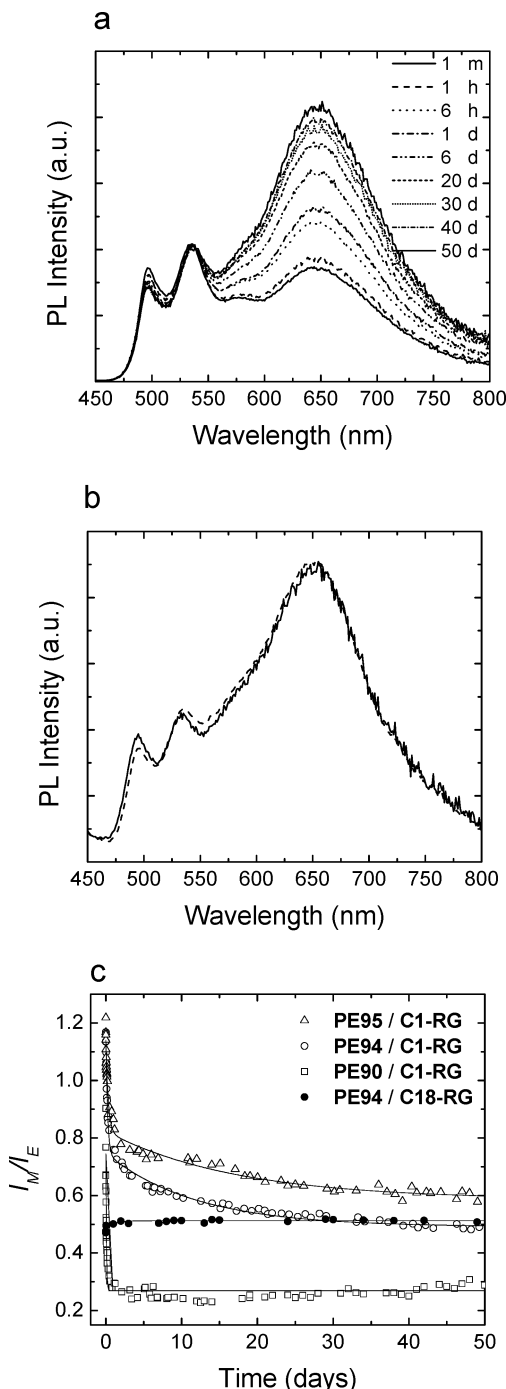


**Figure 2.** (a) PL emission spectra of a quenched blend film containing 0.15% w/w **C1-RG** in **PE94** as a function of aging time (as indicated in the figure) at room temperature. The spectra are normalized to the monomer peak at 537 nm. (b) PL emission spectra of a quenched blend film containing 0.4% w/w **C18-RG** in **PE94** initially after quenching (solid line) and after aging at room temperature for 50 days (dashed line). The spectra are normalized to the monomer peak at 537 nm. (c)  $I_M/I_E$  of quenched blend films containing 0.15% w/w **C1-RG** (open symbols) or 0.4% w/w **C18-RG** (closed symbols) in **PE95** ( $\Delta$ ), **PE94** ( $\circ$ ,  $\bullet$ ), and **PE90** ( $\square$ ) as a function of aging time at room temperature. Solid lines are least-square fits to eq 1.

exhibit the same behavior (individual spectra not shown), but the process was found to be slower in the case of **PE95** and faster for **PE90**. To quantify these differences,  $I_M/I_E$  extracted from the individual experiments was plotted as a function of time (Figure 2c). The observed PL color change was found to fit well to single (**PE90**) or double (**PE95** and **PE94**) exponential equations of the type

$$I_M/I_E = I_{M\infty}/I_{E\infty} + A_1 e^{-t/\tau_1} + A_2 e^{-t/\tau_2} \quad (1)$$

where  $I_{M\infty}/I_{E\infty}$  is  $I_M/I_E$  after aging to equilibrium,  $t$  is the aging time in days, and  $A_1$ ,  $A_2$ ,  $\tau_1$ , and  $\tau_2$  are constants representing the magnitude ( $A$ ) and rate ( $1/\tau$ ) of the PL color change. The data extracted from these fits (Table 1) reveal that a decrease of the matrix crystallinity leads to a decrease of  $I_{M\infty}/I_{E\infty}$ ,  $\tau_1$ , and  $\tau_2$  and an increase of  $A_1$  and  $A_2$ . In other words, the rate at which the dye aggregates and the extent of aggregation (and perhaps the aggregate size) increase with decreasing polymer crystallinity. This observation is in agreement with the increased amount of amorphous phase with decreasing crystallinity and reflects an increase of the dyes' (translational) mobility. In **PE95** and **PE94** blends with **C1-RG** the color change was sufficiently slow to discern two different processes that lead to a decrease of  $I_M/I_E$ . The excimer formation of cyano-OPVs in solid polymer matrices is concomitant with the formation of (electronic) ground state aggregates, and thus the biexponential nature of the aging process points to two different factors that limit the dyes' aggregation rate. The process is consistent with a nucleation process that is followed by a slower aggregate (or crystal) growth that involves diffusion of the dye molecules through the tortuous semicrystalline environment.

To shed more light on the origin of the biexponential aggregation process, and surmising that the aggregation behavior of **C18-RG** in PE might be rather different than that of **C1-RG** (vide supra), we repeated the aging study with binary blends of all the PEs and 0.4% w/w **C18-RG** (i.e., at a similar molar concentration as the 0.15% w/w **C1-RG** blends studied). Interestingly, the dye aggregation appeared to be instantaneous in all samples involving **C18-RG**. Data for the 0.4% w/w **PE94/C18-RG** blend are shown as an example in Figure 2b,c. The emission spectrum of a freshly quenched film (Figure 2b) is virtually identical to that of an aged 0.15% w/w **PE94/C1-RG** film (Figure 2a), and no significant change could be discerned over the course of up to 50 days (Figure 2b,c).<sup>27</sup> Thus, we have found that (i) the length of the rigid cores of **C18-RG** and **C1-RG**, which dominate the total molar volume, are identical (leading to presumably similar diffusion characteristics in a given PE matrix), (ii) the aggregation of **C18-RG** was instantaneous in all polymer matrices employed, (iii) that  $I_{M\infty}/I_{E\infty}$  of about equimolar **PE94/C18-RG** and **PE94/C1-RG** blends are similar, which suggests that the same level of aggregation is reached, and (iv) the alkyl tails are well-known to enhance nucleation (vide supra). Together, these findings support the hypothesis that distinctive aggregation characteristics of **C1-RG** and **C18-RG** in PE matrices are caused by a significantly higher nucleation rate of **C18-RG**. The absence of a pronounced diffusion-related component in the case of the aggregation of **C18-RG** suggests that a large fraction of the dye molecules participates in the nucleation step, leading to the formation of many small aggregates. The process is equally rapid in the different PE hosts employed, suggesting that the aggregation process (and therefore the aggregate size) is relatively independent of the host polymer's crystallinity. The comparably inefficient nucleation of **C1-RG**, in turn, appears to limit the number of dye aggregates formed, leading to slow growth of larger aggregates (or crystals) via diffusion of the dye molecules. The observation of different dye aggregate sizes in blends comprising **C1-RG** and **C18-RG** (by atomic force microscopy, vide infra) further supports this interpretation.

**Deformation-Induced Emission Color Changes in Polyethylene/Cyano-OPV Blend Films.** We reported earlier that (aged) **PE94/C1-RG** blends change their PL emission charac-

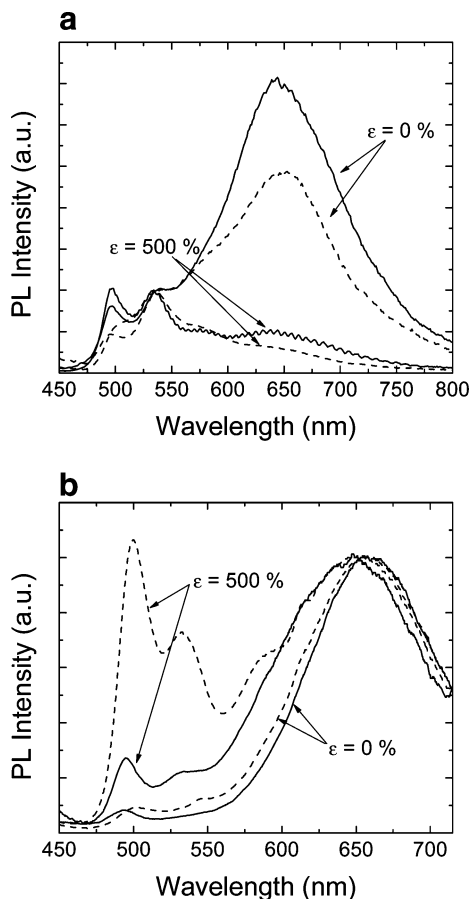


**Figure 3.** PL emission spectra of quenched blend films containing 0.19% w/w **C1-RG** (solid lines) or 0.4% w/w **C18-RG** (dashed lines) in **PE95** (a) or **PE90** (b) at 0 and 500% strain. The spectra are normalized to the monomer peak at 537 nm (a) and excimer peak at ca. 650 nm (b).

**Table 1. Constants Determined by Fitting the Data Shown in Figure 2c to Eq 1**

polymer	$I_M/I_{E\infty}$	$A_1$	$\tau_1$ (days)	$A_2$	$\tau_2$ (days)
<b>PE95</b>	0.58	0.32	0.31	0.24	17.2
<b>PE94</b>	0.49	0.40	0.22	0.26	11.7
<b>PE90</b>	0.27	0.50	0.08		

teristics from excimer-dominated to monomer-rich emission upon deformation beyond the yield point.<sup>2</sup> This color change was ascribed to breakup of nanoscale dye aggregates and the transformation of the phase-separated polymer/dye blend into an apparent molecular dispersion or solution.<sup>2,28</sup> With the above-documented differences in the aggregation behavior of **C1-RG** and **C18-RG** in mind, and the objective to gain further insights into the mechanism of the deformation-induced color change, we conducted a systematic series of optomechanical experiments using a modified rheometer in connection with a PL spectrometer (see Experimental Section for details). This setup enabled us to conduct combined stress-strain-PL measurements by maintaining the center of the stretch zone in a fixed location, which allowed the emission characteristics to be monitored in situ.

We first compared the characteristics of binary blends of **PE94** containing 4  $\mu\text{mol/g}$  of **C1-RG** (0.18% w/w, this system was studied previously<sup>2</sup>) or **C18-RG** (0.4% w/w). The PL spectra of unstretched films comprising **C1-RG** and **C18-RG** (Figure 3a; strain  $\epsilon = l/l_0 - 1 = 0\%$ ) show similar features and are dominated by excimer emission. Tensile deformation has a pronounced effect on the emission spectra of both systems. Upon

deformation to a strain  $\epsilon = 500\%$  (i.e., to a point where necking had occurred) films of both compositions changed their emission color from orange to green. This transformation can be followed in detail in the PL spectra, which display a significant change in the relative intensities of monomer ( $\lambda_{\text{max}} = 495, 537 \text{ nm}$ ) and excimer emission ( $\lambda_{\text{max}} = 650 \text{ nm}$ ). In fact, the stretched samples are dominated by monomer emission and  $I_M/I_E$  increased by an order of magnitude (Figure 3a).

Interestingly, significant differences were found when comparing the mechano-optical response of binary blends of **PE90** containing the same molar concentration of **C1-RG** (0.19% w/w) or **C18-RG** (0.4% w/w). Figure 3b shows the PL emission spectra<sup>29</sup> of the two films at 0 and 500% strain. As can be seen, the emission spectrum of the **C1-RG** blend film exhibits only minor changes upon deformation. By contrast, the sample containing **C18-RG** develops a substantial (1 order of magnitude) increase in  $I_M/I_E$  upon stretching. This difference is another piece of evidence for the hypothesis that the dye aggregates formed in the **PE90/C1-RG** blend are larger than those formed in **PE94/C1-RG** and **PE90/C18-RG** and are therefore difficult to disperse upon deformation.

On the basis of the above-discussed findings, which reflect a preferred aggregation/dispersion behavior of **C18-RG** compared to **C1-RG**, we elected to focus further experiments on the mechanochromic response of PE blends comprising **C18-RG**. We first revisited the aspect of dye solubility and the effect of dye concentration on the mechanochromic response. Consistent with previous findings by our group<sup>2,3</sup> and others,<sup>30–33</sup> PL emission spectra of unstretched **PE94/C18-RG** blend films containing between 0.1 and 0.8% w/w dye show a decrease of  $I_M/I_E$  with increasing **C18-RG** concentration (Figure 4a,b). While films comprising 0.1 or 0.2% w/w of the dye display a prominent monomer contribution, the emission spectra of samples containing 0.4% w/w or more **C18-RG** are dominated by excimer emission. Figure 4b shows the visual appearance of these films under illumination with UV light as a result of deformation just beyond the yield point. All films exhibit an increase of the green monomer fluorescence upon stretching. The visual contrast between stretched and unstretched portions appears to be most pronounced for the 0.4% w/w blend (Figure 4b), which appear to offer the best combination of high initial excimer contribution and good aggregate dispersibility. A set of *uncorrected*, unnormalized PL emission spectra that was obtained in an *in-situ* optomechanical experiment by stretching a sample of this composition to different strains is shown as an example in Figure 4c. The spectra show a substantial increase of the absolute intensity of the monomer band that comes at the expense of the intensity of the excimer band. The change is gradual, and an isoemissive point is observed at ca. 575 nm. This spectral feature is characteristic of two components that are in mutual dependence and confirms that the observed color change is indeed due to excimer to monomer conversion.<sup>34,35</sup>

$I_M/I_E$  values extracted from *in-situ* optomechanical experiments of unstretched **PE94/C18-RG** blend films containing between 0.1 and 0.8% w/w dye are plotted along with stress against strain in Figure 4d. The stress-strain profiles for all samples are qualitatively the same, showing yielding, neck propagation, and strain hardening features characteristic of this PE grade.<sup>36</sup> Interestingly, the shape of the  $I_M/I_E$ -strain traces, while differing in magnitude between samples, all display similarities to the stress-strain profiles, which were hitherto not observed.  $I_M/I_E$  values exhibit a steep increase upon yielding (Figure 4e), increase only moderately during neck

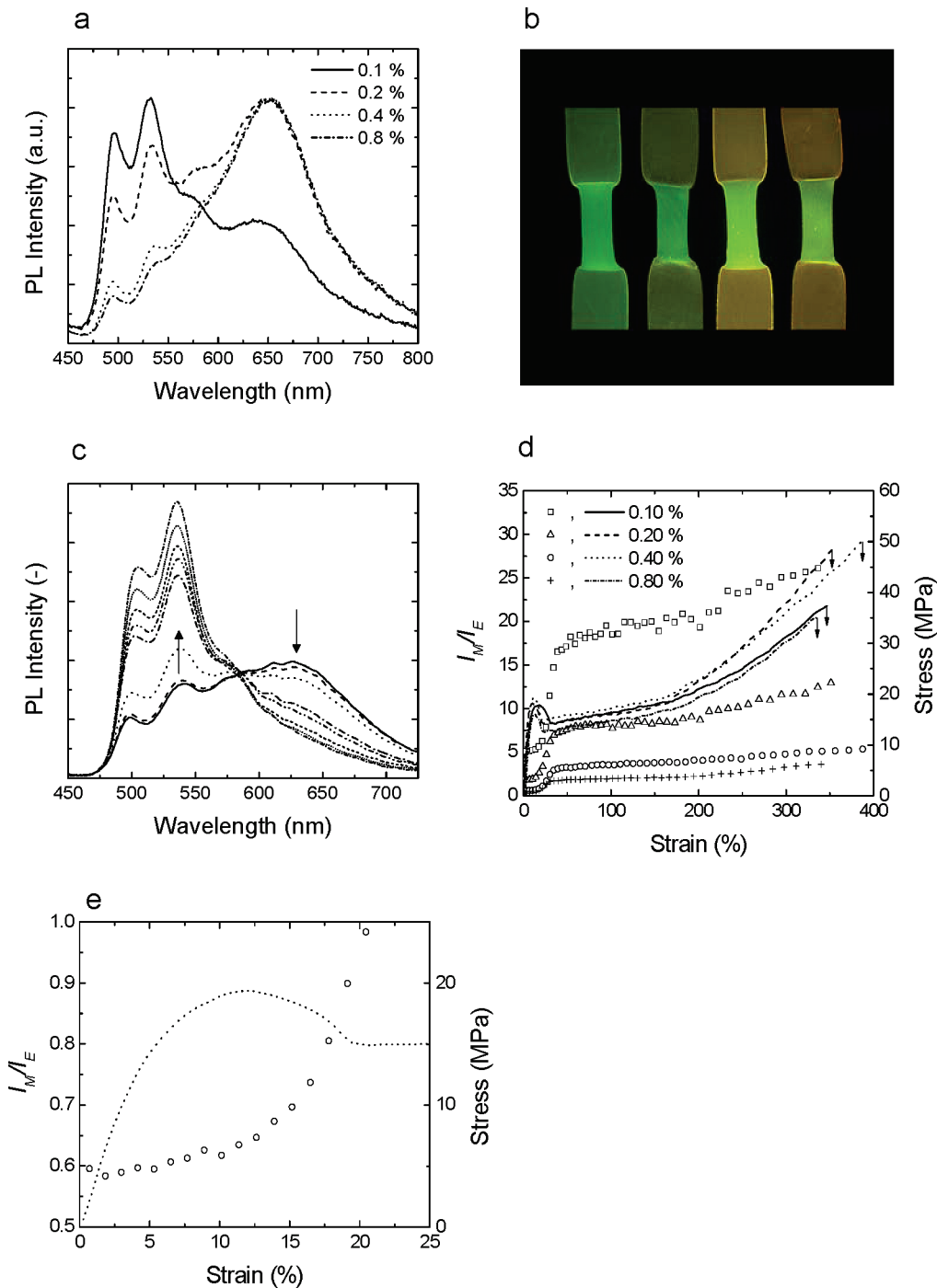


**Figure 4.** Properties of quenched blend films of **PE94** and 0.1, 0.2, 0.4, or 0.8% w/w **C18-RG**. (a) PL emission spectra of pristine films. The spectra are normalized to the maximum value. (b) Picture of films deformed to  $\epsilon = l/l_0 - 1 = \sim 300\%$ . The wide regions are strained portions that had not necked. (c) Uncorrected PL emission spectra (not normalized) of a quenched blend film of **PE94** and 0.4% w/w **C18-RG** as a function of strain to break; arrows indicate direction of change in spectra. (d)  $I_M/I_E$  (symbols, measured at 540 and 650 nm) and tensile stress (lines) as a function of strain for blends between **PE94** and between 0.1 and 0.8% w/w **C18-RG**. (e) Magnification of the data for the 0.4% w/w **PE94/C18-RG** blend shown in (d) in the necking region.

propagation, and display a slightly steeper increase during strain hardening. Blends featuring low dye concentration exhibit larger *absolute* changes of  $I_M/I_E$  than materials with high concentration of dye. Upon deformation to a strain of ca. 300%,  $I_M/I_E$  of blend films containing 0.1% dye reaches a value of ca. 25, which is identical to the  $I_M/I_E$  observed for **C18-RG** in dilute chloroform solution. This indicates that virtually all dye aggregates have been disintegrated during deformation and that the dye is molecularly dissolved or dispersed at this stage. Lower values of  $I_M/I_E$  were observed in the stretched portions of blend films with a higher concentration of the dye (Figure 4d),

indicating an incomplete breakup of the aggregates upon deformation. This is most likely due to the larger initial size of the aggregates in the higher concentration blends (vide infra). A comparison of the  $I_M/I_E$  values with the pictures shown in Figure 4b shows, however, that  $I_M/I_E$  is not necessarily a good representation of the perceived visual contrast. Normalization for the different initial excimer contributions allows one to express the *relative* changes observed in the samples upon deformation in an appropriate manner. For example, the ratios of  $I_M/I_E$  after deformation to 50% strain (i.e., just beyond the yield point) to the initial values of  $I_M/I_E$  are 3.4, 4.2, 5.3, and

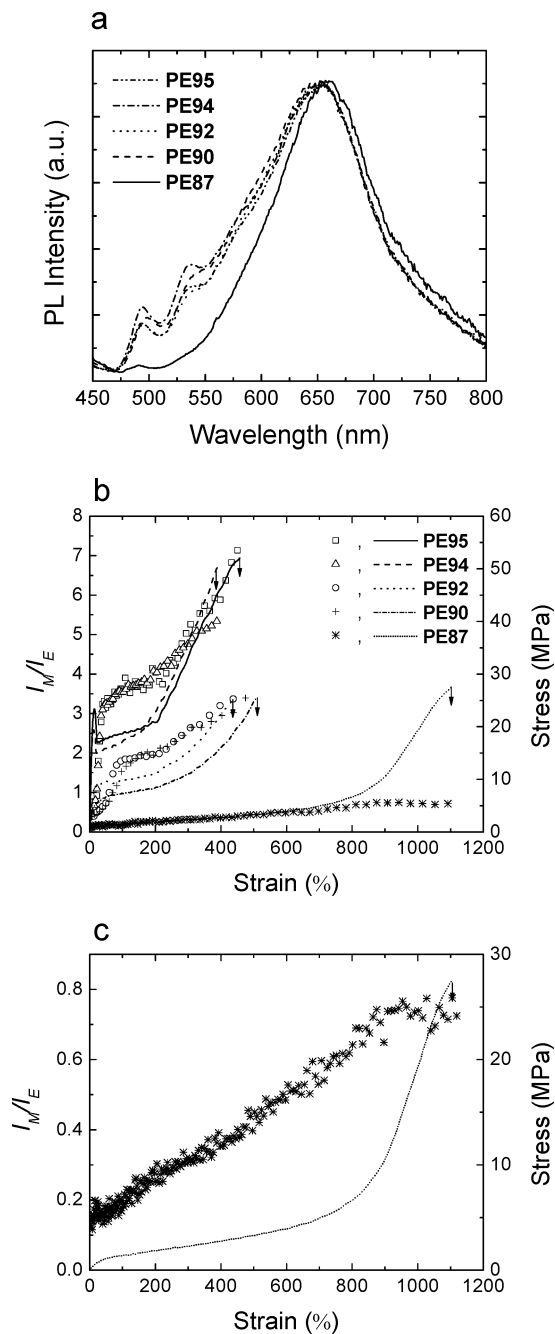


**Figure 5.** (a) PL emission spectra of quenched blend films of **PE95**, **PE94**, **PE92**, **PE90**, and **PE87** containing 0.4% w/w **C18-RG**. The spectra are normalized to the excimer peak at ca. 650 nm. (b)  $I_M/I_E$  (symbols, measured at 500 and 650 nm) and tensile stress (lines) as a function of strain for the same. (c) Magnification of the data shown in (b) for the **PE87/C18-RG** blend.

4.0 for blends containing 0.1%, 0.2%, 0.4%, and 0.8% w/w **C18-RG**, respectively. Comparison of this data with Figure 4b indicates that the best contrast is achieved in the 0.4% w/w blend. It appears that there is an optimum dye concentration that leads to materials which are initially dominated by excimer emission ( $I_M/I_E < 1$ ) but transform to a system that is rich in monomer emission ( $I_M/I_E > 1$ ) upon deformation. Below this optimal dye concentration, the materials feature a higher level of monomer emission in the unstretched state, which reduces the attainable color contrast. An increase of the dye concentration above this optimal level does not change the emission spectra of unstretched films significantly (as can be seen from the spectra of the 0.4%, and 0.8% w/w blends shown in Figure

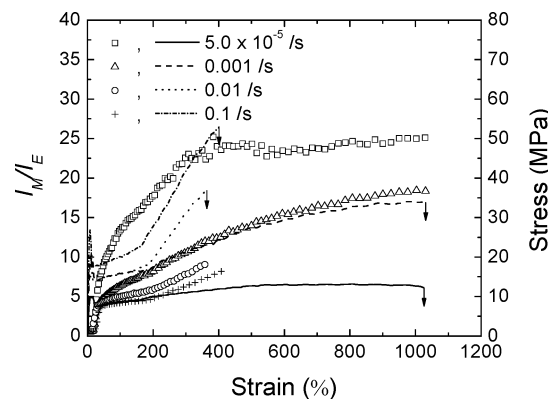


**Figure 6.**  $I_M/I_E$  (symbols, measured at 500 and 650 nm) and tensile stress (lines) as a function of strain for blends between **PE95** measured at strain rates between 0.1 and  $5.0 \times 10^{-5} \text{ s}^{-1}$ .

4a), but it may lead to larger aggregates that are more difficult to disperse.

We next conducted a series of experiments that probe the effect of polymer crystallinity on the mechanochromic response of PE/C18-RG blends. The PL emission spectra of freshly quenched blend films of **PE95**, **PE94**, **PE92**, **PE90**, or **PE87** and 0.4% w/w **C18-RG** are all dominated by excimer emission (Figure 5a). The **PE87** blend shows almost no monomer emission, indicating that virtually all of the dye molecules are in an aggregated state. This is consistent with the low crystallinity/high free volume of this polymer, which leads to a high translational mobility of the dye molecules and facilitates aggregation. All other blend films display PL spectra that feature clearly detectable monomer emission bands. The  $I_M/I_E$  values of these samples are virtually identical, and it appears that in these hosts a similarly small fraction of the dye molecules is molecularly dispersed within the polyethylene matrix. This is consistent with the higher crystallinity/lower free volume in these materials, which prevent complete aggregation. Interestingly, the similar  $I_M/I_E$  values observed for **PE95**, **PE94**, **PE92**, and **PE90** blends containing 0.4% w/w **C18-RG** suggest that the difference in crystallinity does not significantly influence the fraction of dye molecules that remain molecularly incorporated within the polyethylene matrix.

Tensile deformation of these PE/C18-RG blends led to an increase of  $I_M/I_E$  in all samples investigated. Figure 5b shows that the extent of color change exhibits a significant dependence on the host polymer's crystallinity. The  $I_M/I_E$ -strain traces of **PE95**, **PE94**, **PE92**, and **PE90** blends all display striking similarities to the stress-strain profiles. In these cases  $I_M/I_E$  exhibits a steep increase upon yielding (Figure 5b), increases moderately during neck propagation, and displays a slightly steeper increase during strain hardening. Blends of **PE95** or **PE94** (vide supra) are virtually identical and show the largest color change. **PE92** and **PE90** blends appear to form another “group”, where a somewhat less pronounced color change is observed. The **PE87** blend, featuring primarily an elastic stress response, shows a very modest linear increase in  $I_M/I_E$  with strain, even at high strains where a large stress increase is observed (Figure 5c). The data suggest that the mechanochromic effect observed in the different blends studied is directly related to the microstructure of the PE.<sup>19,42</sup> Pronounced changes of  $I_M/I_E$  can be observed for blends of polymers that adopt lamellar morphologies (**PE95**, **PE94**, **PE92**, and **PE90**). By contrast, the elastomeric **PE87** forms almost exclusively fringed micellar type crystals, and blends based on this host show only a minor mechanochromic response.

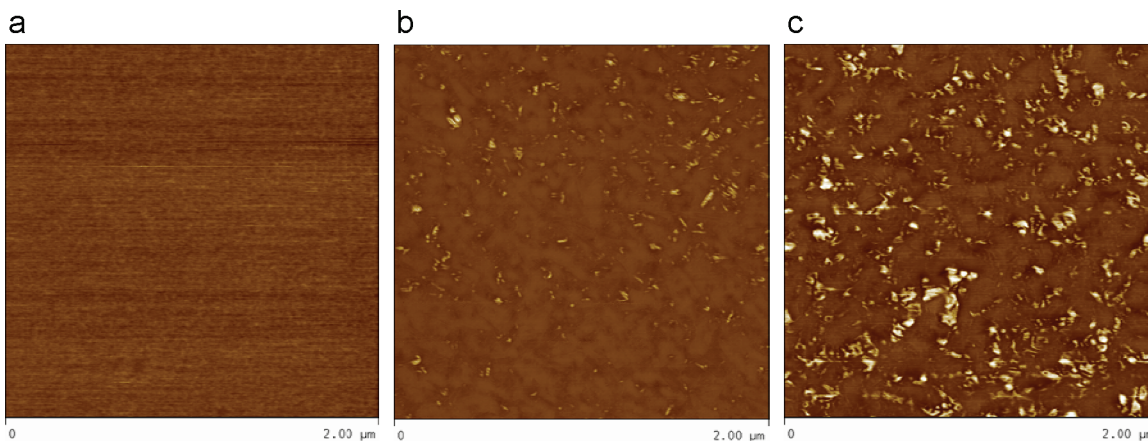


**Figure 7.** AFM micrographs displaying free surfaces of quenched films of **PE87** containing 0% (a), 0.4% (b), and 1.0% w/w **C18-RG** (c).

A quantitative difference exists for the mechanochromic response of blends comprising the higher density **PE95** or **PE94**, which both exhibit thick crystalline lamellae, and the lower density **PE92** or **PE90**, in which the lamellae are much thinner and less abundant. Thus, from a mechanistic aspect, it appears that the ability of the polymer host to disperse dye aggregates upon deformation is primarily related to the plastic deformation process of the PE crystallites, specifically those arranged in a lamellar morphology. Data from the low-strain (elastic) regime of **PE95**, **PE94**, **PE92**, and **PE90** blends and the  $I_M/I_E$ –strain trace of **PE87** reflect that elastic deformation, which primarily involves the extension of chains in the amorphous region, apparently has little effect on the dispersion of dye aggregates. The absence of significant changes in the inelastic regime of **PE87**, in which plastic deformation occurs primarily via attachment and detachment of short crystallizable chain segments,<sup>38</sup> further suggests that crystallographic slip processes, which are the dominant mechanism involved in the plastic deformation of high crystallinity materials,<sup>39–42</sup> play an important role in the mechanically induced dispersion of the excimer-forming sensor molecules. These findings are consistent with the mechanochromic responses of other recently investigated materials.<sup>3,4</sup> For example, blends created from semicrystalline poly(ethylene terephthalate) exhibit a significant color change upon deformation, whereas the mechanochromic response of an otherwise identical material based on the fully amorphous poly(ethylene terephthalate glycol) is much less pronounced.<sup>3</sup> Similarly, blends between thermoplastic polyurethanes and **C18-RG** showed very little color change upon deformation, and it was necessary to covalently incorporate the dye molecules into the polymer backbone in order to achieve a significant mechanochromic response.<sup>4</sup>

Since the PE/cyano-OPV blends are displaced from a thermodynamic equilibrium upon deformation, another important question, addressed only qualitatively here, is how well the color is retained after deformation. Gratifyingly, when stored under ambient conditions, the emission spectra of the drawn portions of **PE95** and **PE94** blends containing either **C1-RG** or **C18-RG** remain unchanged almost indefinitely, which is important from a technological point of view. This observed stability of the dispersed polymer/dye blend points to a considerably reduced translational mobility of the dye upon stretching, which may be attributed to transformation of crystalline regions from lamellar to fibrillar structure of higher crystallinity,<sup>43</sup> a reduction in free volume hole size,<sup>44–46</sup> and/or an increase of internal crystal interfacial area,<sup>47–49</sup> which may all play a role in stabilizing the molecularly mixed systems. The emission spectra of the drawn portions of blends based on

**PE92**, **PE90**, or **PE87** and **C18-RG**, in turn, displayed a decrease of  $I_M/I_E$  over time, suggesting reaggregation of the dye molecules. The speed and extent of the change of  $I_M/I_E$  were qualitatively found to scale with decreasing crystallinity. In blends of **PE87** the minor contribution of monomer emission generated upon deformation was found to completely fade within seconds. These observations are consistent with the increase in guest molecule mobility observed in PE with decreasing crystallinity.

Finally, we probed the influence of strain rate on the mechanochromic response of blend films comprising **PE95** and 0.4% w/w **C18-RG**. Blend films were subjected to tensile deformation at strain rates between 0.1 and  $5.0 \times 10^{-5} \text{ s}^{-1}$ . The resulting stress–strain– $I_M/I_E$  traces are shown in Figure 6. The stress profiles show a decrease in the yield stress and ultimate stress with decreasing rate, consistent with the increase in viscous flow expected at low rates of strain.<sup>50–55</sup> Interestingly, the magnitude of the color change, and therewith the extent of aggregate breakup, follows an opposite trend and increases with decreasing strain rate. As can be seen from Figure 6, the  $I_M/I_E$ –strain trace of the blend strained at  $0.1 \text{ s}^{-1}$  is similar to those shown above, and the sample fails before the aggregates are completely dispersed ( $I_M/I_E \sim 8$ ). In contrast,  $I_M/I_E$  of the blend strained at  $5.0 \times 10^{-5} \text{ s}^{-1}$  increases steeply with strain and levels off at a value of ca. 25 (indicating complete dispersion of the dye aggregates, *vide supra*) long before this sample breaks. This response may reflect the strain rate dependence of the host viscoelasticity. Alternatively, the crystalline morphology evolution with strain may depend on strain rate, this in turn influencing the dispersion of dye aggregates. Discernment among these possibilities requires *in-situ* observations beyond the scope of the present study.

**Atomic Force Microscopy.** To gain further evidence regarding the size of the dye aggregates formed, atomic force microscopy (AFM, tapping mode) was used to investigate the morphological properties of selected PE/cyano-OPV blends before and after deformation. Initial studies were performed with **PE87**; this polymer was selected because the absence of large PE crystallites allowed for an unambiguous identification of dye aggregates. Figure 7 shows a series of phase images of compression-molded surfaces of **PE87** and **PE87/C18-RG** blends containing 0.4 or 1.0% w/w dye.<sup>56</sup> The images clearly reveal that the dimensions of the dye aggregates formed are at the nanometer length scale. The largest aggregates found in the 0.4 and 1.0% w/w blends are of a length of about 80 and 180 nm, respectively, confirming the proposed increase of aggregate size with increasing dye concentration. With the notions that **PE87** blends display only a very limited mechanochromic

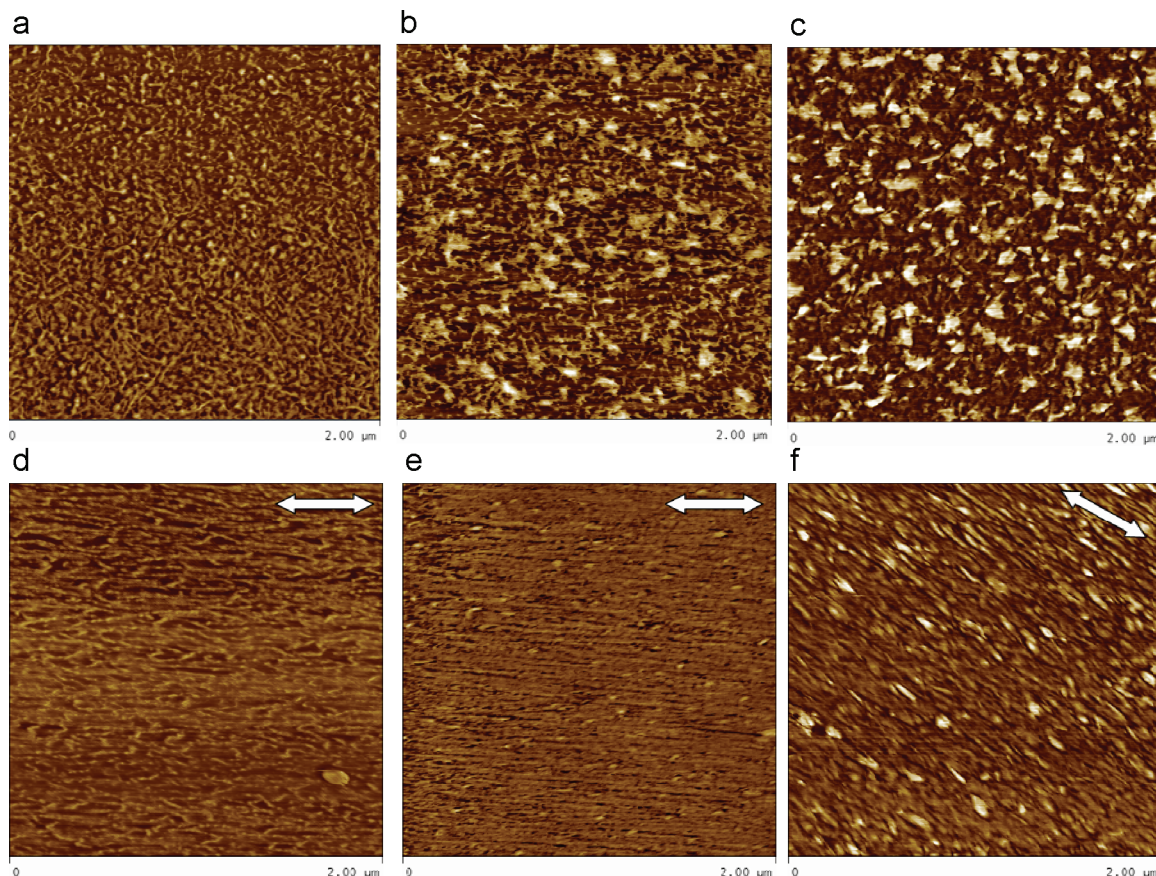


**Figure 8.** AFM micrographs displaying free surfaces of quenched films of **PE90** containing 0% (a, d), 0.4% (b, e), and 1.0% w/w **C18-RG** (c, f) before (upper) and after (lower) deformation to  $\epsilon = l/l_0 - 1 = 200\%$ .

response and rapid dye reaggregation (vide supra) and that dye aggregates are exceedingly difficult to discern in the higher density PE samples, **PE90** was employed to investigate the influence of tensile deformation on blend morphology. Figure 8 shows phase images of compression-molded surfaces of **PE90** and **PE90/C18-RG** blends containing 0.4 or 1.0% w/w dye before (top) and after (bottom) deformation of the blends to a strain of 200%. The “background” of the PE crystals limits the accuracy with which the aggregate size in these blends can be established, but it appears that the maximum length (100 and 150 nm for 0.4 and 1.0% w/w blends) and number of aggregates in unstretched **PE90** is comparable to those in **PE87** blends at the same concentration, although the aggregates appear to be of lower aspect ratio in **PE90** than in **PE87**. The AFM images show that uniaxial deformation of the films leads to the conversion of the PE crystallites into fibrillar structures that are primarily oriented along the stretch direction. At the same time, the number and size of the dye aggregates are reduced. This effect is particularly pronounced in the 0.4% w/w blend, consistent with the smaller initial aggregate size in this material and the results of our mechanochromic studies, in which incomplete aggregate breakup was documented for samples of higher dye concentration. The fact that the dye aggregates observed in blends of **PE87** (which display only a modest mechanochromic response) and **PE90** (in which the mechanochromic response is more pronounced) are of similar size corroborates our conclusion that *both* small aggregates *and* the presence of lamellar PE crystals are required to maximize the mechanochromic response. Finally, Figure 9 shows AFM phase images of a 0.19% w/w **PE90/C1-RG** blend film before and after deformation to a strain of 200%. This comparative experiment (cf. Figure 8b,e) unequivocally demonstrates that,

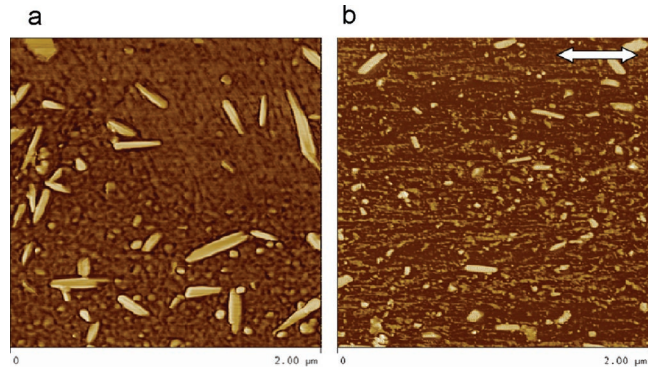


**Figure 9.** AFM micrographs displaying free surfaces of quenched films of **PE90** containing 0.4% w/w **C1-RG** before (a) and after (b) deformation to  $\epsilon = l/l_0 - 1 = 200\%$ .

at least in this host and using identical processing protocols, **C1-RG** indeed forms microscopic crystals that are much larger than the aggregates observed in the case of **C18-RG**, which is consistent with our postulate of slower nucleation. Figure 9 further shows that deformation of the 0.19% w/w **PE90/C1-RG** blend film leads to fracture of the dye crystals, but it appears that a large fraction of the crystalline dye remains phase-separated from the PE host, consistent with the very limited mechanochromic response of this blend (Figure 3b). This effect may be less important in the higher crystallinity matrices (Figure 3a), where the reduced translational mobility of the dye molecules leads to the creation of smaller crystals.<sup>2</sup>

## Conclusions

In summary, we have demonstrated that in blends between PE and excimer-forming cyano-OPV dyes the extent of color

change observed upon deformation, and thus the ability of the polymer host to break up dye aggregates, is primarily influenced by three parameters: dye aggregate size, polymer crystallinity, and strain rate. The nucleation rate of dye aggregates, and therewith the size of the aggregates, can be controlled via the nature of the groups attached to the dye. In particular, the introduction of long aliphatic groups leads to much higher nucleation rates, which promotes the formation of small aggregates. Low dye concentrations also lead to small aggregates which are readily broken up upon tensile deformation of a high crystallinity PE. Larger aggregates (formed at high dye concentrations or at slow nucleation rates) are not readily dispersed. This mechanically induced dispersion of the excimer-forming sensor molecules upon deformation is shown to be related to the *plastic* deformation process of PE crystallites, specifically those arranged in a lamellar morphology, and thus increases with increasing polymer crystallinity. Deformation of polymer blends that do not exhibit lamellar morphologies does not lead to significant changes in color. Finally, in high-density materials the magnitude of the color change, and therewith the extent of aggregate breakup, was shown to increase with decreasing strain rate. This behavior may be due to variation in viscoelastic response of the host polymer with strain rate.

**Acknowledgment.** We gratefully acknowledge financial support from the National Science Foundation (CW: NSF DMI-0428208; PTM: CTS-0552414). The authors thank Dr. I. Manas and K. Chung for stimulating discussions and J. Kunzelman for technical assistance.

**Supporting Information Available:** Solubility plots of **C18-RG** in **PE94**; pictures and graphs illustrating the development of strain during tensile experiments. This material is available free of charge via the Internet at <http://pubs.acs.org>.

## References and Notes

- (1) Löwe, C.; Weder, C. *Adv. Mater.* **2002**, *14*, 1625.
- (2) Crenshaw, B. R.; Weder, C. *Chem. Mater.* **2003**, *15*, 4717.
- (3) Kinami, M.; Crenshaw, B. R.; Weder, C. *Chem. Mater.* **2006**, *18*, 946.
- (4) Crenshaw, B.; Weder, C. *Macromolecules* **2006**, *39*, 9581.
- (5) Kunzelman, J.; Crenshaw, B. R.; Kinami, M.; Weder, C. *Macromol. Rapid Commun.* **2006**, *27*, 1981.
- (6) Förster, T.; Kasper, K. Z. *Phys. Chem. (Muenchen, Ger.)* **1954**, *1*, 275.
- (7) Förster, T.; Kasper, K. Z. *Elektrochem. Angew. Phys. Chem.* **1955**, *59*, 976.
- (8) In line with common practice, the term “monomer” is used to describe emission from single-molecule excited states, as opposed to excimers.
- (9) Löwe, C.; Weder, C. *Synthesis* **2002**, 1185.
- (10) Gill, R. E.; van Hutten, P. F.; Meetsma, A.; Hadzioannou, G. *Chem. Mater.* **1996**, *8*, 1341.
- (11) Döttinger, S. E.; Hohloch, M.; Hohnholz, D.; Segura, J. L.; Steinhuber, E.; Hanack, M. *Synth. Met.* **1997**, *84*, 267.
- (12) Hohloch, M.; Maichle-Moessmer, C.; Hanack, M. *Chem. Mater.* **1998**, *10*, 1327.
- (13) Oelkrug, D.; Tompert, A.; Gierschner, J.; Egelhaaf, H.-J.; Hanack, M.; Hohloch, M.; Steinhuber, E. *J. Phys. Chem. B* **1998**, *102*, 1902.
- (14) Henari, F. Z.; Manaa, H.; Kretsch, K. P.; Blau, W. J.; Rost, H.; Pfeiffer, S.; Teuschel, A.; Tillmann, H.; Hörhold, H. H. *Chem. Phys. Lett.* **1999**, *307*, 163.
- (15) van Hutten, P. F.; Krasnikov, V. V.; Brouwer, H. J.; Hadzioannou, G. *Chem. Phys.* **1999**, *241*, 139.
- (16) de Souza, M. M.; Rumbles, G.; Gould, I. R.; Amer, H.; Samuel, I. D. W.; Moratti, S. C.; Holmes, A. B. *Synth. Met.* **2000**, *111–112*, 539.
- (17) Martinez-Ruiz, P.; Behnisch, B.; Schweikart, K. H.; Hanack, M.; Luer, L.; Oelkrug, D. *Chem.—Eur. J.* **2000**, *6*, 1294.
- (18) Freudenmann, R.; Behnisch, B.; Hanack, M. *J. Mater. Chem.* **2001**, *11*, 1618.
- (19) Bensason, S.; Minick, J.; Moet, A.; Chum, S.; Hiltner, A.; Baer, E. *J. Polym. Sci., Part B: Polym. Phys.* **1996**, *34*, 1301.
- (20) Wunderlich, B. *Macromolecular Physics*; Academic Press: New York, 1980; Vol. 3, p 42.
- (21) Sentmanat, M. L. *Rheol. Acta* **2004**, *43*, 657.
- (22) Turnbull, D. *J. Appl. Phys.* **1949**, *20*, 817.
- (23) Turnbull, D. *J. Chem. Phys.* **1952**, *20*, 411.
- (24) Turnbull, D. *Solid State Phys.* **1956**, *3*, 225.
- (25) Turnbull, D.; Cormia, R. L. *J. Chem. Phys.* **1961**, *34*, 820.
- (26) Huang, J.; Lu, W.; Bartell, L. S. *J. Phys. Chem.* **1996**, *100*, 14276.
- (27) Some variation was observed in the value of  $I_M/I_E$  (which in the absence of the ageing effect is equal to  $I_{M\infty}/I_{E\infty}$ ) for different 0.4% w/w **PE94/C18-RG** samples. This variation appeared to be caused by variations of the (rather high) quenching rate, which could not be very well controlled.
- (28) Trabesinger, W.; Renn, A.; Hecht, B.; Wild, U. P.; Montali, A.; Smith, P.; Weder, C. *J. Phys. Chem. B* **2000**, *104*, 5221.
- (29) These spectra were taken *in situ* and corrected for detector response.
- (30) Avis, A.; Porter, G. *J. Chem. Soc., Faraday Trans. 2* **1974**, *70*, 1057.
- (31) Johnson, G. E. *Macromolecules* **1980**, *13*, 839.
- (32) Szadkowska-Nicze, M.; Wolszczak, M.; Kroh, J.; Mayer, J. *J. Photochem. Photobiol. A* **1993**, *75*, 125.
- (33) Spies, C.; Gehrke, R. *J. Phys. Chem. A* **2002**, *106*, 5348.
- (34) Lehr, B.; Egelhaaf, H. J.; Rapp, W.; Bayer, E.; Oelkrug, D. *J. Fluoresc.* **1998**, *8*, 171.
- (35) Förster, T. *Angew. Chem.* **1969**, *81*, 364.
- (36) The apparent strain at which these samples break ( $\sim 350\%$ ) is somewhat smaller than the strain calculated by the displacement of ink marks on the samples ( $\sim 500\%$ ). This artifact is due to the high strain reached during the initial yield and the fixed region wherein strain occurs (see Supporting Information for details).
- (37) Flory, P. J. *J. Am. Chem. Soc.* **1962**, *84*, 2857.
- (38) Bensason, S.; Stepanov, E. V.; Chum, S.; Hiltner, A.; Baer, E. *Macromolecules* **1997**, *30*, 2436.
- (39) Peterlin, A. *J. Mater. Sci.* **1971**, *6*, 490.
- (40) Peterlin, A. *Colloid Polym. Sci.* **1987**, *265*, 357.
- (41) Lin, L.; Argon, A. S. *J. Mater. Sci.* **1994**, *29*, 294.
- (42) Hiss, R.; Hobeika, S.; Lynn, C.; Strobl, G. *Macromolecules* **1999**, *32*, 4390.
- (43) Wang, C.; Xu, J.; Weiss, R. G. *J. Phys. Chem. B* **2003**, *107*, 7015.
- (44) Naciri, J.; Weiss, R. G. *Macromolecules* **1989**, *22*, 3928.
- (45) Dong, H.; Jacob, K. I. *Macromolecules* **2003**, *36*, 8881.
- (46) Monge, M. A.; Diaz, J. A.; Pareja, R. *Macromolecules* **2004**, *37*, 7223.
- (47) Jang, Y. T.; Phillips, P. J.; Thulstrup, E. W. *Chem. Phys. Lett.* **1982**, *93*, 66.
- (48) Parikh, D.; Phillips, P. J. *J. Chem. Phys.* **1985**, *83*, 1948.
- (49) Phillips, P. J. *Chem. Rev.* **1990**, *90*, 425.
- (50) Brown, N.; Ward, I. M. *J. Mater. Sci.* **1983**, *18*, 1405.
- (51) Lu, X.; Wang, X.; Brown, N. *J. Mater. Sci.* **1988**, *23*, 643.
- (52) Zhou, Y.; Brown, N. *J. Mater. Sci.* **1989**, *24*, 1458.
- (53) Egan, B. J.; Delatycki, O. *J. Mater. Sci.* **1995**, *30*, 3307.
- (54) Shah, A.; Stepanov, E. V.; Capaccio, G.; Hiltner, A.; Baer, E. *J. Polym. Sci., Part B: Polym. Phys.* **1998**, *36*, 2355.
- (55) Nitta, K. H.; Ishiburo, T. *J. Polym. Sci., Part B: Polym. Phys.* **2002**, *40*, 2018.
- (56) The apparent volume fraction of dye observed in the AFM images is significantly higher than it would be observed in a single plane due to the deep penetration of the AFM tip into the soft material.

MA062936J